Journal of Chromatography A, 652 (1993) 283–289
Elsevier Science Publishers B.V., Amsterdam

CHROM. 25 306

Dispersion in capillary electrophoresis with external flow control methods

Catherine A. Keely, Robert R. Holloway, Tom A.A.M. van de Goor and Douglass McManigill*

Hewlett Packard Laboratories, 3500 Deer Creek Road, P.O. Box 10350, Palo Alto, CA 94303-0867 (USA)

ABSTRACT

Recently, methods for controlling the bulk flow of the buffer which are independent of the electrophoretic migration have been demonstrated in capillary electrophoresis (CE) systems. These methods include controlling the electroosmosis by radially directed electric fields, and controlling the bulk flow by siphoning. This paper investigates basic dispersion mechanisms at work by examining the dispersion of dimethyl sulfoxide under various external control methods. It is found that the electroosmotic flow control methods exhibit the same dispersive behavior as the conventional CE system. In particular, the results for pH 7 buffers obey the theoretical expression for the plate height in all configurations. However, in all configurations, pH 2.7 buffers do not follow the theory, and counter to intuition, additional pressure can improve the plate height at pH 2.7. Taking all these methods together, one can develop a technique to appropriately adjust the electrophoretic and bulk flow to optimize resolution.

INTRODUCTION

Capillary electrophoresis (CE) makes use of electroosmotic flow (EOF) and electrophoretic migration induced by a strong electrical field along the axis of the capillary [1,2]. Traditionally these two transport mechanisms were linked because one could not be adjusted by external means without affecting the other. However, in the past few years it has been observed that an external *radial* field can significantly affect the electroosmotic flow while electrophoretic migration remains dependent only on the axial field [3–5]. Adjustment of the radial field allows electroosmotic flow to be increased, decreased, or even reversed. Since electrophoretic migration depends only on the axial field, it is not influenced by the radial adjustment. The EOF control serves to set the bulk flow so that the sample is held in the column to increase resolution, or is flushed through to increase speed. Thus, the electroosmotic and electrophoretic velocities can be adjusted independently.

In CE, electroosmosis generates bulk flow. A pressure differential can also be used to generate bulk flow. Models for the flow profile resulting from EOF and pressure driven flow have been derived [6–8], and from the flow profile an expression for the plate height (height equivalent to a theoretical plate, or HETP) has been formed [7,8] as a measure of system efficiency.

This paper compares the plate height theory with the experimental results of CE systems using three methods of bulk flow control, which include radial field methods and pressure driven flow. It is found that the pH of the buffer–electrolyte solution has a significant impact on the plate height in all systems, yet is not accounted for in the flow profile models or the resulting plate height expression. It is further shown that because of this pH effect, using pressure-driven flow with electroosmosis can actually improve the plate height in many cases.

* Corresponding author.

0021-9673/93/$06.00

Electroosmotic flow control

In 1989, Lee *et al.* [3] and Ghowsi and Gale [5] independently introduced the concept of constraining the electrical field in the radial direction as a means of controlling the EOF without affecting the electrophoretic migration rate. One advantage of such a system would be the ability to perform different kinds of separations on the same capillary where otherwise capillaries of different lengths might be required in order to be time efficient. Another advantage would be the ability to program the fields to optimize the separation at each subsection of an electropherogram. The approach was demonstrated to effectively adjust the bulk velocity over a wide range when using low-pH buffers, but the effectiveness diminishes as pH values increase [9].

The above advantages of external flow control could also be realized by simply pressure driving the bulk flow [10], which is also independent of the electrophoretic migration. However, this option is not always useful because of the extra dispersion caused by the resulting Hagen–Poiseuille velocity profile. The velocity profile resulting from controlling the EOF by radial fields is not currently known, but it is usually assumed to be mostly plug flow as is normally generated by EOF at small dimensions [6]. Chien and Helmer [11] and Towns and Regnier [12] have described profiles when the flow is perturbed by other means, and their findings may be related to the EOF controlled profiles.

This paper studies two separate configurations for controlling EOF via radial fields, in addition

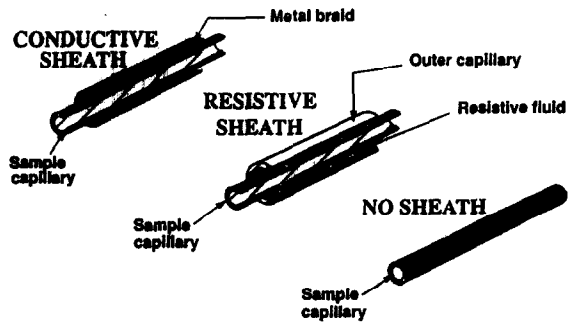

Fig. 1. General capillary configurations used: conductive sheath made by threading capillary through metal webbing; resistive sheath made by surrounding capillary by resistive fluid; and no sheath.

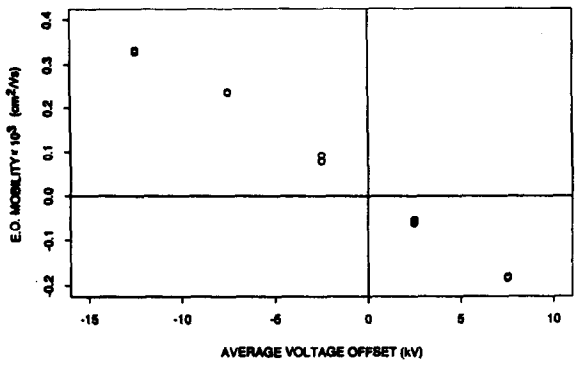

Fig. 2. Electroosmotic (E.O.) mobility plotted as a function of average voltage offset of conductive sheath [$V_{sheath} - (V_{inlet} + V_{outlet})/2$]. Conditions: capillary length 65.5 cm to detector, conductive sheath covering 70%, phosphate buffer pH 2.7, 170 V/cm axial field.

to a conventional configuration. Fig. 1 shows these three configurations schematically. The first method constrains the radial electric field by placing a conductive coating or jacket around the outside of the capillary and holding it at a uniform voltage or ground [9], thus producing a radial field that varies along the length of the capillary. A demonstration of the velocity control possible by radial field adjustment with phosphate buffer pH 2.7 is shown by Fig. 2 where the electroosmotic mobility of dimethyl sulfoxide (DMSO) is plotted as a function of the average voltage difference between the conductive jacket and the buffer fluid. The second method constrains the radial field by placing a resistive coating or fluid around the capillary and holding the ends at specific voltages to create a uniform radial field across the capillary wall everywhere along the capillary [3,9,13]. Conventional systems do not explicitly constrain the radial field, although objects near the capillary, *e.g.* detectors, may affect it.

THEORETICAL MODEL

Datta and Kotamarthi [7] developed a model for dispersion when both electroosmotic flow and Poiseuille flow exist, using the electroosmotic velocity profile developed by Rice and Whitehead [6]. From this model, an expression for plate height H (or HETP) can be written as:

$$H = \frac{2D}{v_{tot}} + \frac{a^2}{24Dv_{tot}} \cdot (v_p^2 + \delta_2 v_p v_e + \delta_3 v_e^2) \quad (1)$$

where

$$\delta_2 = \frac{1}{48} \cdot \frac{\eta}{(1-\eta)} \cdot \left[\frac{1}{12} - \frac{2}{(\kappa a)^2} + \frac{16}{(\kappa a)^4}\left(\frac{1-\eta}{\eta}\right)\right]$$

$$\delta_3 = \frac{1}{48} \cdot \frac{\eta^2}{(1-\eta)^2} \cdot \left[\frac{3}{8} + \frac{2}{(\kappa a)^2} - \frac{1}{\eta(\kappa a)^2} - \frac{1}{\eta^2(\kappa a)^2}\right]$$

$$\eta = \frac{2}{\kappa a} \cdot \frac{I_1(\kappa a)}{I_0(\kappa a)}$$

and where D is the diffusion coefficient, v_{tot} is the total average velocity, a is the capillary inside radius, v_p is the Poiseuille flow velocity component, v_e is the electroosmotic flow velocity component, κ^{-1} is the double layer thickness, and $I_n(x)$ is the modified Bessel function of the first kind, order n. Note how the δ terms depend on the parameter κa, which is the ratio of the capillary radius to the double layer thickness, and the terms are negligible for values of $\kappa a >$ 200. For ionic strengths ranging from 1 to 100 mM, the double layer thickness κ^{-1} ranges from 10 nm to 1 nm [14,15]. Thus, under normal CE conditions, capillary diameters greater than about 4 μm reduce the plate height expression to

$$H = \frac{2D}{v_{tot}} + \frac{a^2}{24Dv_{tot}} v_p^2 \quad (2)$$

This formula has also been derived by Grushka [8].

One extreme of this expression occurs when there is no Poiseuille velocity component, or $v_p = 0$, and the equation reduces to the familiar diffusion limited dispersion. The other extreme occurs when the total velocity results from pure Poiseuille flow, or $v_{tot} = v_p$, and then the last term becomes linearly related to the velocity.

EXPERIMENTAL

Apparatus

Fig. 3 schematically shows the apparatus used in the plate height experiments. As described above and shown in Fig. 1, three capillary configurations were used: a conductive sheath, a resistive sheath, and a configuration with no sheath used as a reference. For the conductive sheath, the capillary was threaded through a metal braid which covered 56% of the capillary length. The 50 μm I.D. × 180 μm O.D. fused-silica capillary used in the experiments (Polymicro Technologies, Phoenix, AZ, USA) was typically 40 cm long, with a detector window 16.5 cm from the inlet. The inlet side was connected to a high-voltage supply (Spellman High Voltage, Plainview, NY, USA), and the outlet end and the sheath were both typically connected to ground, but for certain experiments one or the other were connected to a second high-voltage supply. The conventional "no-sheath" configuration was identical except that the metal braid was removed.

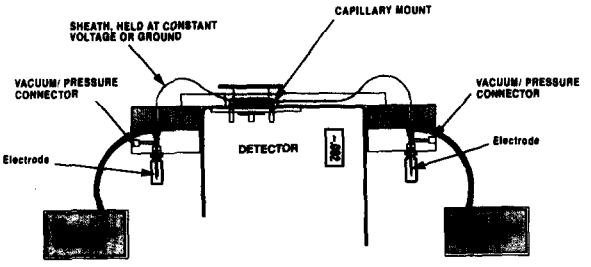

Fig. 3. Capillary electrophoresis apparatus used in experiments. Shown with conductive sheath. HV = High voltage.

For the resistive sheath, the method of Lee *et al.* [3] was used in which the sample capillary rests inside a second capillary filled with a resistive buffer, allowing a constant field to be held across the wall of the inner capillary. The inner capillary dimensions were as stated above, and the outer capillary dimensions were 540 μm I.D. × 680 μm O.D., and 22.5 cm long centered lengthwise along the inner capillary.

A UV absorbance detector (Linear Instruments, Reno, NV, USA) set to 210 nm was used to detect the sample front. A window was burned in the polyimide coating of the capillaries for UV transmission.

In the pressure-driven flow experiments, pressure was connected to ports indicated in Fig. 3 and controlled by an in-house designed pressure regulator. The pressure was adjusted to be 10, 20

or 30 cmH_2O (1, 2 or 3 kPa, respectively) and it was connected to one side or the other of the CE system to push with or against the EOF.

Chemicals

DMSO (Alltech, Deerfield, IL, USA) was normally used as the neutral molecule under study. For a few experiments, mesityl oxide (Aldrich, Milwaukee, WI, USA) and benzene (Aldrich) were substituted for DMSO. The background buffer was 10 m*M* phosphate buffer with 0.5% DMSO, and the run was made using a front of the same 10 m*M* phosphate buffer with 1% DMSO. Certain experiments used 10 m*M* glycine buffer instead of phosphate. The outer capillary in the resistive sheath system contained 1 m*M* phosphate buffer pH 2.8.

Phosphate buffers at pH 2.7 were prepared by titrating 10 m*M* phosphoric acid (J.T. Baker, Jackson, TN, USA) to pH 2.7 with 50% sodium hydroxide (J.T. Baker), resulting in a nominal ionic strength of 7.8 m*M*. The alternative glycine buffer was prepared by titrating 10 m*M* glycine (Bio-Rad, Richmond, CA, USA) to pH 2.7 with concentrated hydrochloric acid (Fluka, Ronkonkoma, NY, USA), the final ionic strength being 5.1 m*M*. Phosphate buffers at pH 7 were made by titrating 10 m*M* monobasic potassium phosphate (J.T. Baker) with 4 *M* potassium hydroxide (Fluka) to pH 7, resulting in an ionic strength of 17.7 m*M*. The pH 8.6 glycine buffer was made from the pH 2.7 glycine buffer by titration with 50% sodium hydroxide, producing an ionic strength of 6.0 m*M*.

Procedure

The background buffer contained DMSO to eliminate any skew in the front caused by adsorption-desorption to the wall of the capillary. Frontal analysis was used to eliminate the additional variance of the injection, and the detector variance was assumed to be negligible. An in-house program using standard formulas and S-Plus (Statistical Sciences, Seattle, WA, USA) operations was used to calculate statistical moments of the UV absorbance signal. The program would take the derivative of the raw signal, trim the data to an approximately 6σ wide region centered on the peak, smooth the data, and perform a moments analysis to obtain the length-based variance σ^2. This variance was related to the experimental plate height,

$$H = \frac{\sigma^2}{l}$$

where l is the capillary length from the inlet to the detector.

RESULTS AND DISCUSSION

Configuration study

Results of the experiments are in the form of plate height (10^{-6} m) *versus* velocity (10^{-3} m/s) plots (H–u curves). The first set of experiments compared the behavior of the three configurations with a pH 2.7 buffer and with a pH 7 buffer. Fig. 4 shows these results, along with the

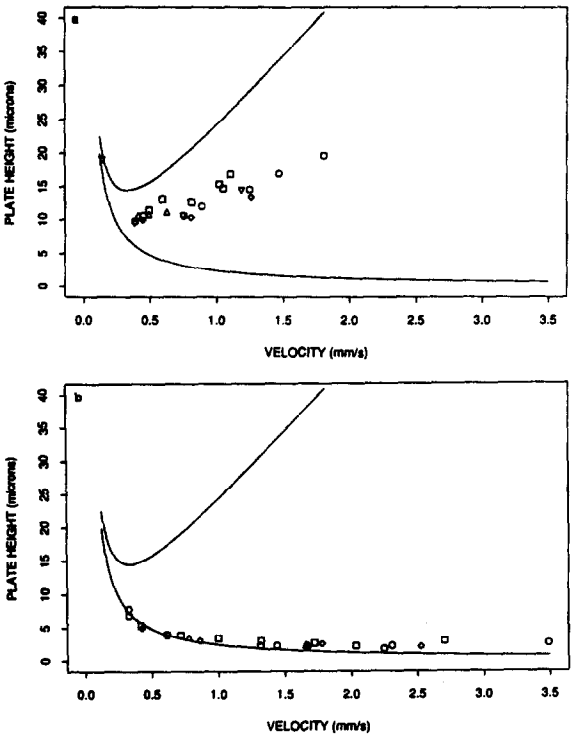

Fig. 4. Plate height *vs.* velocity for three configurations. Theoretical curves are for diffusion-limited dispersion (lower curve) and pressure-limited dispersion (higher curve). ○ = Conductive sheath and phosphate buffer; △ = resistive sheath and phosphate buffer; □ = no sheath and phosphate buffer; ◇ = no sheath and glycine buffer; ▽ = conductive sheath and glycine buffer. (a) Buffer pH 2.7; (b) buffer pH 7.

theoretical curve for diffusion limited dispersion, and the curve for pure pressure-driven flow, the extremes of eqn. 2. Note that in all configurations the pH 7 buffer data points fall on the diffusion limit line, while the pH 2.7 data points ascend at about 70% of the pressure limit level. This is contrary to theoretical expectations. Glycine buffer substituted for phosphate buffer produced the same results. Although not shown here, samples which used mesityl oxide and benzene as the neutral molecule also gave similar results.

Experiments were also run with two smaller diameter capillaries. As Fig. 5 shows, the theoretical pressure limit curve is different for each capillary, yet as in the original case, it can still be seen that the observed plate heights rise as the velocity increases.

Relating the results to the EOF control, it is seen that the EOF control methods do not cause any significant additional dispersion compared to the conventional no-sheath configuration. The pH was the only parameter which caused a change in the dispersion behavior, but at this time we have no plate height expression that describes this pH dependence. Temperature gradients were examined as a possible cause, but were found to be insignificant. It should be recalled that the radial field EOF control methods also have a pH dependence, in that the velocity adjustment range is large with low-pH buffers but minimal with high-pH buffers. Thus, the phenomena that allows control may also perturb the velocity profile, but actively controlling EOF does not seem to affect the resulting plate height–velocity relationship.

Pressure study

Fig. 6 shows data taken at pH 7 with a 20 cmH_2O head (20 mbar or 2 kPa) attached at the capillary inlet or outlet. The range of experimental velocities was obtained by varying the axial field and by changing the direction, but not magnitude, of the pressure head. Overlaid on the data is the diffusion limit curve, and the theoretical plate height curve determined by eqn. 2 with v_p obtained by the Hagen–Poiseuille law [16]. Because the v_p term is squared, its contribution to the plate height is not dependent on direction, and thus experiments could be made with the pressure head pushing in either direction. As can be seen, the data points follow the plate height theory very well.

The implications of the plate height theory are demonstrated more graphically by Fig. 7. This plot shows a series of runs all taken under identical electrical conditions, but with varying amounts of applied pressure. It can be seen that with a given axial field, pressure may be used to increase or decrease the bulk flow velocity with a minor increase in plate height. Since the data obey eqn. 2, it follows that added pressure will not cause as great an increase in plate height

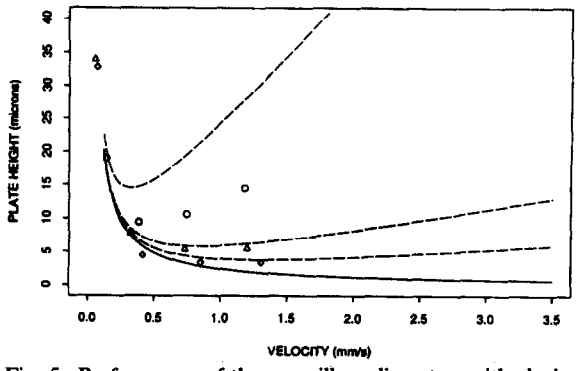

Fig. 5. Performance of three capillary diameters with glycine buffer pH 2.7. Three upper dashed theoretical curves are for pressure-limited dispersion corresponding to the three diameters. Lowest curve is for diffusion-limited dispersion. ○ = 50 μm I.D.; △ = 20 μm I.D.; ◇ = 13 μm I.D. Conditions: axial field varied, conductive sheath.

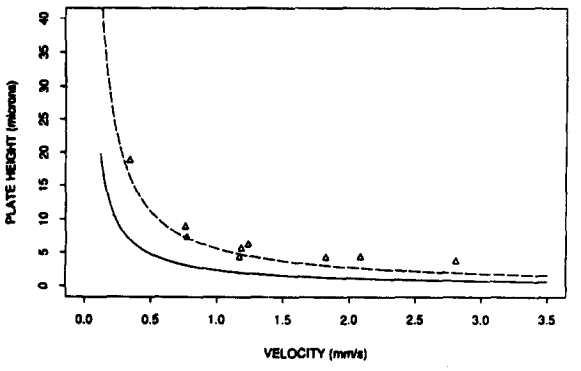

Fig. 6. Phosphate buffer pH 7 with 20 cmH_2O head attached to inlet or outlet end of capillary during run. Dashed curve is eqn. 2 with v_p corresponding to a 20 cmH_2O head. Lower curve is diffusion-limited dispersion. Conditions: axial field varied, conductive sheath.

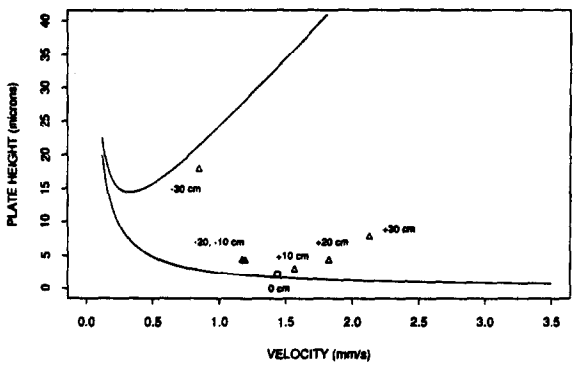

Fig. 7. Phosphate buffer pH 7 with 250 V/cm axial field. ○ = No pressure head; △ = additional pressure head varied from −30 cmH_2O to +30 cmH_2O (−3 kPa to +3 kPa). Conditions: constant axial field, conductive sheath.

when smaller diameter capillaries are used. On the other hand, when larger molecules are used (lower D), the added pressure will cause a more significant plate height increase [8].

Fig. 8 illustrates the data from a similar experiment using the pH 2.7 buffer. The ascending data points (open circles) are from Fig. 4 and show the trend when there is no pressure applied. The main data points (△) show the effect of changing pressure using a constant axial field. As is clear, additional pressure in the direction of the bulk flow improves the plate height over that obtained for the same velocity without the use of pressure. In fact, the minimum of the curve of data points obtained with the same

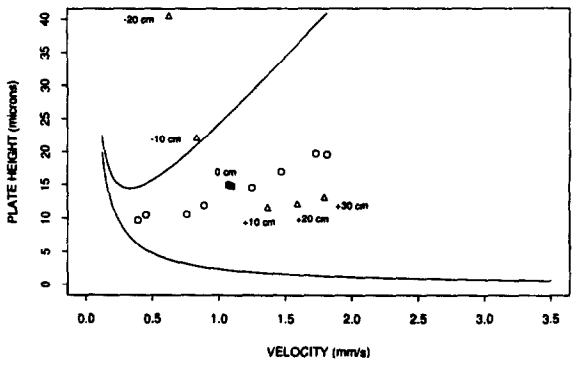

Fig. 8. Phosphate buffer pH 2.7 with applied pressure. ○ show the trend of data with no applied pressure, radial and axial field varied. △ are points where pressure is varied from −20 cmH_2O to +30 cmH_2O (−2 kPa to +3 kPa) while the axial field remains constant at 500 V/cm. Conditions: conductive sheath.

voltage settings occurs when pressure is added.

These results seem to indicate that at pH 2.7 there is some type of disturbance of the velocity profile that is not quite normal Poiseuille flow and acts against the bulk flow. Transient effects of the sudden voltage initiation have been ruled out as a cause.

CONCLUSIONS

Plate height *versus* velocity curves have been used to examine the performance of different external flow control methods. It has been found that radial field EOF control methods do not change the plate heights relative to the conventional no-sheath configuration. In all cases, pH 7 buffers follow the diffusion limit theory. When pressure is added, pH 7 buffers continue to follow the theory containing the additional pressure driven flow term. The theory and data also predict that pressure may be useful to adjust the bulk flow velocity with a small increase in plate height.

A pH 2.7 the EOF methods do not change the plate height, but all configurations produce data fitting between the diffusion limit and the pure pressure driven limit. We do not have an expression to predict this pH dependency. However, the plate height can be improved by adding pressure in the direction of bulk flow, thus the implication that at pH 2.7 there is a back flow.

ACKNOWLEDGMENT

The authors wish to acknowledge and thank Jim Young for his contribution to this work.

REFERENCES

1 J.W. Jorgenson and K.D. Lukacs, *Anal. Chem.*, 53 (1981) 1298.
2 F.E.P. Mikkers, F.M. Everaerts and Th.P.E.M. Verheggen, *J. Chromatogr.*, 169 (1979) 11.
3 C.S. Lee, W.C. Blanchard and C.-T. Wu, *Anal. Chem.*, 62 (1990) 1550.
4 C.S. Lee, D. McManigill, C.-T. Wu and B. Patel, *Anal. Chem.*, 63 (1991) 1519.
5 K. Ghowsi and R.J. Gale, in R.P. Buck (Editor), *Proceedings of the International Symposium on Biosensor Technology 1989*, Marcel Dekker, New York, 1990, pp. 55–62.

6 C.L. Rice and R. Whitehead, *J. Phys. Chem.*, 69 (1965) 4017.
7 R. Datta and V.R. Kotamarthi, *AIChE J.*, 36 (1990) 916.
8 E. Grushka, *J. Chromatogr.*, 559 (1991) 81.
9 R.R. Holloway, C.A. Keely, J.A. Lux, D. McManigill and J.E. Young, presented at the *4th International Symposium on High Performance Capillary Electrophoresis, Amsterdam, February 9–13, 1992*, poster PT-27.
10 F.M. Everaerts, T.P.E.M. Verheggen and J.L.M. van de Venne, *J. Chromatogr.*, 123 (1976) 139.
11 R.-L. Chien and J.C. Helmer, *Anal. Chem.*, 63 (1991) 1354.
12 J.K. Towns and F.E. Regnier, *Anal. Chem.*, 64 (1992) 2473.
13 M.A. Hayes and A.G. Ewing, *Anal. Chem.*, 64 (1992) 512.
14 P.C. Hiemenz, *Principles of Colloid and Surface Chemistry*, Marcel Dekker, New York, 2nd ed., 1986.
15 R.J. Hunter, *Zeta Potential in Colloid Science*, Academic Press, London, 1981.
16 J.C. Giddings, *Unified Separation Science*, Wiley, New York, 1991.